EEET ECOLOGICAL ENGINEERING & ENVIRONMENTAL TECHNOLOGY

Ecological Engineering & Environmental Technology, 2025, 26(9), 138–150
https://doi.org/10.12912/27197050/209229
ISSN 2719–7050, License CC-BY 4.0

Received: 2025.07.21
Accepted: 2025.08.16
Published: 2025.09.01

Modeling the impact of land cover change on erosion dynamics in the Matting River catchment, Saddang Watershed

Mikhael Layuk[1], Andang Suryana Soma[2*], Samuel Arung Paembonan[2]

[1] Forestry Science Study Program Graduate School, Hasanuddin Uiversity, 90224, Makassar, Indonesia
[2] Department of Forestry, Faculty of Forestry, Hasanuddin University, 90245, Makassar, Indonesia
* Correspondence author's email: s_andangs@unhas.ac.id

ABSTRACT

This study aims to evaluate the impact of land cover changes on erosion rates in the Matting River catchment, part of the Saddang watershed in north Toraja regency, and to project future conditions up to 2030. The research follows a remote sensing and modeling approach combining MOLUSCE for land cover change projection and SWAT for erosion simulation. Satellite imagery for 2011 and 2020 were classified and validated using confusion matrices, while land cover for 2030 was projected. These data were used to simulate hydrological and erosion dynamics through the SWAT model. The main findings revealed a significant increase in agricultural land (from 399 ha in 2011 to 519 ha in 2030) and a decline in rice fields and grasslands. This shift directly influenced erosion patterns: total erosion was 1.9 million tons/year in 2011 and declined progressively to 0.5 million tons/year by 2030. Forested and shrub-covered areas contributed the least to erosion, while agricultural lands contributed the most. The projected results indicated that the area is moving towards lower erosion hazard classes, supported by improved land cover and potential conservation actions. This research is limited by the assumption of consistent climatic input and fixed land management practices during the projection period. However, it provides practical value in guiding future land use and conservation planning. The originality of this study lies in its integrated approach using MOLUSCE and SWAT for forecasting land cover-driven erosion at the sub-watershed level, contributing to regional-scale watershed management strategies.

Keywords: land cover, erosion rate, SWAT, MOLUSCE.

INTRODUCTION

Land cover change is one of the main factors influencing erosion rates and watershed degradation, especially in upstream areas. The conversion of forests and natural vegetation into agricultural land or settlements increases surface runoff and sediment production.

In the Saddang watershed – particularly in the Toraja Utara regency – these changes have become increasingly evident. Data from Global Forest Watch show a significant decline in forest area between 2011 and 2020, accompanied by an expansion of agricultural and settlement areas.

Various studies in Indonesia have demonstrated the impact of land use change on erosion, which can be modeled using SWAT. For example, Hidayat and Sulistyo (2019) showed that forest-to-bare land conversion in the upstream area of the Mrica reservoir could increase erosion by up to 82%, although it can be mitigated through land conservation. Nandini et al. (2019), in the Babak watershed (Lombok), also recorded that land use changes affect runoff and sedimentation, modeled using SWAT with adequate statistical validation.

Closer to Sulawesi, Asrianto et al. (2023) examined land cover transformation in the Mamasa Watershed (a sub-watershed of Saddang), finding that secondary forest changes from 2011 to 2020 reflected land cover trends in Toraja Utara and significantly influenced river discharge through SWAT simulations.

In addition, Purwitaningsih et al. (2020) studied land use scenarios in the Kedurus watershed

and found that conservation scenarios could reduce runoff by up to 65% while also lowering flood potential.While these findings illustrate the vast potential of SWAT-based land change modeling, most studies remain retrospective and lack comprehensive integration of future spatial projections in scenario-based erosion simulations.

Geospatial models such as MOLUSCE (modules for land use change evaluation) and SWAT (soil and water assessment tool) offer solutions to bridge this gap. Abbaspour, Vaghefi and Srinivasan (2018) emphasized the importance of spatial calibration and high-quality data in SWAT implementation. This study aims to develop a spatial predictive approach by integrating satellite image-based land cover projections using MOLUSCE and erosion simulations using SWAT in the Matting catchment area. By combining historical analysis with future simulations up to 2030, this research seeks to provide land management recommendations that are adaptive to environmental dynamics.

This study is based on the hypothesis that uncontrolled expansion of agricultural and settlement areas will significantly increase erosion risk by 2030, unless accompanied by spatially and quantitatively appropriate land management strategies. Its primary scientific contribution lies in the development of an integrated modeling framework that produces future erosion risk maps based on scenarios, offering a novel approach to soil conservation and sustainable land use planning in tropical regions with data limitations.

MATERIALS AND METHODS

Study area

The research was conducted in the Matting catchment area, part of the Saddang watershed, located in north Toraja regency, south Sulawesi province. The area is characterized by hilly topography, varied land use, and high rainfall intensity, making it susceptible to erosion (Figure 1).

Land cover analysis

Land cover classification was conducted using Landsat 7 ETM+ and Landsat 8 OLI/TIRS satellite imagery, downloaded from the United States Geological Survey (USGS), covering the study area for the years 2011 and 2020. The imagery had a spatial resolution of 30 meters and was provided in GeoTIFF format. Pre-processing steps included area clipping based on the study boundary, band composition (e.g., RGB and

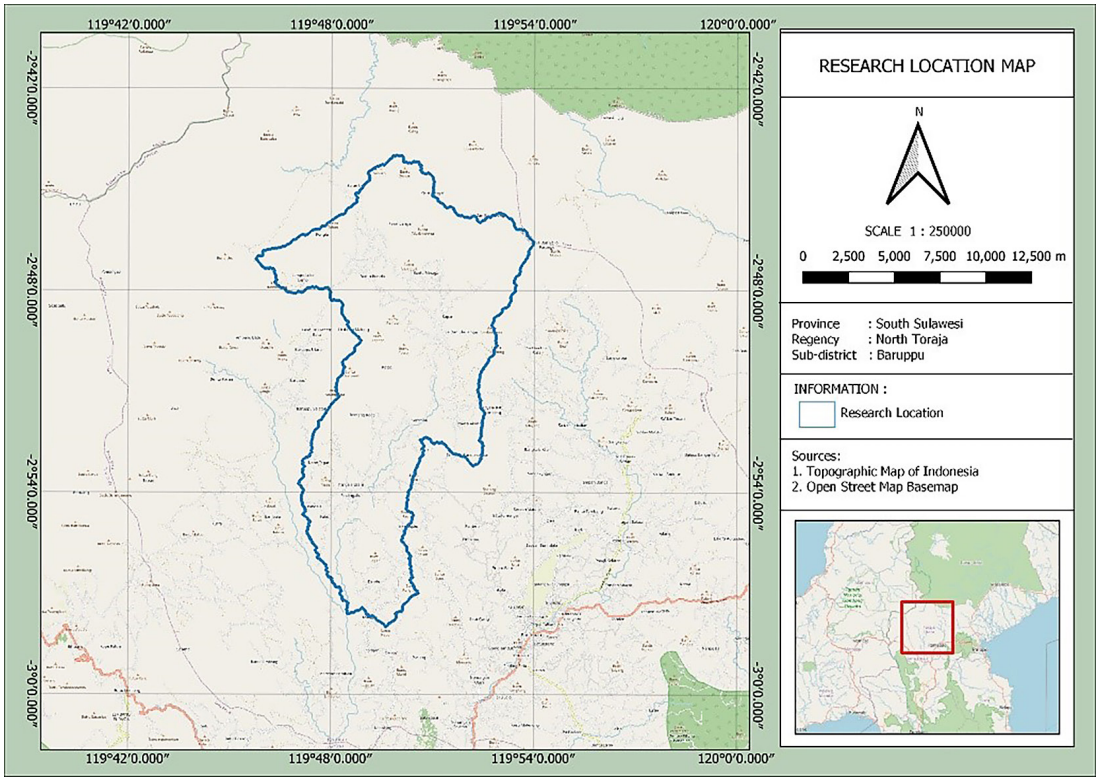

Figure 1. Administrative area of the research site

infrared combinations), and mosaicking to merge multiple scenes where necessary.

The classification was carried out using supervised classification methods via the MOLUSCE plugin in QGIS. This process involved preparing training samples based on visual interpretation and reference land cover maps, selecting classification algorithms such as Random Forest or Neural Network, and producing classified land cover maps according to the Indonesian National Standard (SNI 7645:2010). Land cover change analysis was performed by inputting the two classified maps from 2011 and 2020 into MOLUSCE. In addition, driving factor layers were generated, including slope (derived from 30 m SRTM DEM), distance to roads (based on national road network data), and population density (from BPS – Indonesian Statistics Agency). MOLUSCE was then used to simulate land cover change predictions using algorithms such as artificial neural networks (ANN) and logistic regression.

Model validation was conducted using a confusion matrix and the Kappa coefficient, with Kappa values above 0.6 indicating acceptable predictive reliability. The validated results were utilized to analyze spatial and temporal patterns of land cover transition and to project future land use dynamics. Classification and prediction accuracy were evaluated by comparing results to actual conditions using confusion matrix outputs (see Tables 1 and 2). Kappa value equation (Vieira, 2006):

$$K = \frac{P_0 - P_E}{1 - P_E} \quad (1)$$

where: P_0 – Number of correct classifications divided by the total of all data, PE – Sum of the results times the number of predictions and references per class.

Erosion rate analysis

Geographic information system (GIS) integrated with the SWAT was used to simulate hydrological processes and erosion rates. According to Abbaspour, Vaghefi, and Srinivasan (2018), SWAT is a physically based, process-driven simulation model widely used to predict the impacts of land use and climate variability on the hydrological cycle and sediment transport at the watershed scale. Siregar, Ritung, and Subagyo (2015) also noted that SWAT has been extensively applied

Table 1. Indonesia's national standard land cover classification

No.	Citra class name (classification results)	Cover classes SNI land	Code SNI	Information
1	Dryland forests secondary	Secondary forests	1	Forest cover with disorders human
2	Wetland forests	Swamp forest/primary forest	1	Forest with soil water saturated
3	Shrub	Bush/bushes	2	Secondary vegetation, not tightly closed
4	Open land	Open land	7	Vacant land, former mines, no productive
5	Paddy	Paddy	4	Irrigated rice land or rain catchment
6	Plantation	Plantation	5	Annual commodities: palm oil, rubber,coffee, etc.
7	Settlements	Settlements	8	Developed areas, villages, cities
8	Water	Water Body	9	Rivers, lakes, reservoirs
9	Savannah/Grass	Meadow/Savanna	6	Natural grass, savannah
10	FarmingMix	Agriculture	3	Plant mix food, horticulture, etc.
11	Clouds/Cloud Shadows	Clouds/shadows cloud	10	Cloud-covered areas, cannot classified

Note: Indonesian National Standard, 2010.

Table 2. Confusion matrix (Congalton and Green, 2019)

References/predictions	Land **c**over A	Land **c**over B	Land **c**over C	Total **r**eferences
Land cover A				
Land cover B				
Land cover C				
Total predictions				

across various landscapes in Indonesia to assess erosion risks and hydrological dynamics.

The application of SWAT begins with watershed delineation, where watershed boundaries and river networks are derived from a digital elevation model (DEM) with a spatial resolution of 30 meters, obtained from the united states geological survey (USGS) or the shuttle radar topography mission (SRTM) via the EarthExplorer platform. Subsequently, hydrologic response units (HRUs) are defined through the overlay of land use, soil type, and slope data, enabling spatially distributed hydrological simulations.

The model requires several key input datasets. Topographic characteristics are derived from the DEM; soil texture and erodibility data are sourced from global soil maps provided by the food and agriculture organization (FAO) and supplemented with national data from the Indonesian Ministry of Agriculture. Daily climate data—including precipitation, temperature, solar radiation, wind speed, and relative humidity—are obtained from the Meteorology, Climatology, and Geophysics Agency (BMKG).

Land cover information is generated from Landsat 7 imagery for 2011 and Landsat 8 imagery for 2020, classified using supervised classification techniques in QGIS software with the assistance of the MOLUSCE plugin. The selection of these two years was based on the availability of consistently cloud-free imagery and the representativeness of the time interval for capturing significant land use change dynamics over the past decade.

Once all input data are processed and prepared, the model is configured through the SWAT interface, and simulations are run to estimate key hydrological components such as surface runoff, soil erosion (sediment yield), evapotranspiration, and water balance over the specified time period. Where available, observational data are used to calibrate and validate the model with the help of the SWAT-CUP tool, thereby improving the reliability of the simulation results. Ultimately, the calibrated SWAT model is employed to analyze various land cover change scenarios and to evaluate their impact on hydrological processes and erosion risks at the watershed scale with the development of equation models.

Equation of surface flow value (Soulis, 2021):

$$Q_{surf} = \frac{(R-0.2S)^2}{(R+0.8S)} \quad (2)$$

where: *Qsurf* – surface flow (mm), *R* – daily rainfall (mm), *CN* – curve number – depending on the type of soil and land cover, *S* – maximum groundwater retention potential (mm).

Equation of erosion rate value (Neitsch et al., 2011):

$$Sed = 11.8 \times (Q_{surf} \times q_{peak} \times HRU\ area)\ 0.56 \times \times K \times C \times P \times LS \quad (3)$$

where: *Sed* – sediment load (tons), *Qsurf* – surface flow (mm), *Qpeak* – peak flow discharge (m³/s), area, *HRU – HRU area* (ha), *K* – soil erodibility factor, *LS* – length and slope factor, *C* – land cover factor, *P* – conservation factor.

Displaying erosion rate values along with the classification of erosion hazard classes in a watershed spatial analysis has an essential purpose, especially in the context of planning and managing land and water resources (Ministry of Environment and Forestry, 2019). The erosion rate values obtained from models such as SWAT provide quantitative information on the amount of soil loss (in tons/ha/year) due to erosion processes in a specific area (Cheng, 2017). However, these figures are not informative enough if they are not further interpreted in the form of hazard categories or classes. Therefore, classifying erosion rates into erosion hazard classes is crucial, as it enables stakeholders to understand, communicate, and utilize the analysis more easily as a basis for informed decision-making (Utomo and Arsyad, 2020). The classification of erosion hazard classes generally follows a standard based on annual erosion rate values, which are divided into five main classes (Dharmawan, 2023):

- Class I (very light): < 15 tons/ha/year,
- Class II (Light): 15–60 tons/ha/year,
- Class III (Medium): 60–180 tons/ha/year,
- Class IV (weight): 180–480 tons/ha/year,
- Class V (very heavy): > 480 tons/ha/year.

RESULTS AND DISCUSSION

Land cover analysis

The analysis of land cover change was carried out via the MOLUSCE plugin in the QGIS software, which uses baseline data from 2011 and 2020. For 2030, it involves projecting future land

cover change patterns on the basis of historical trends in land cover change. On the basis of the results of the land cover analysis, several data points related to land cover changes were obtained, as shown in Table 3.

The change in land cover in the table above shows significant changes in the time span of 2011, 2020, and 2031, such as land cover in the form of forests, which in 2011 had an area of 53 Ha; however, in 2020, it increased to 54 Ha, such that in the pattern of land cover changes that occurred, it can be projected that land cover changes from 2031--62 Ha, whereas for agricultural land cover in 2011, it has a relatively low area value of 399 Ha. However, in 2020, it increased to 442 Ha. However, in the projected land cover for 2031, it increased to 519 Ha, and in 2020, it increased to 416 Ha. Specifically, in 2011, it had an area of 366 Ha, whereas in 2021, it became 327 Ha. In 2011, it had a projected land cover in 2031, it decreased to 281 Ha. This also happened to land cover in the form of grassland. In 2011, it had an area of 416 Ha, and in 2021, it also occurred in the form of grasslands. In 2011, it had an area of 416 Ha. In 2011, it had an area of 416 Ha, and in 2011, it had an area of 416 Ha, and, The results of the land cover analysis that were carried out through molluskes have an overall kappa validation value of 0.66, with a match percentage of 75.27% with the transition matrix as follows (Figure 2 and Table 4).

An overall accuracy value of 74% shows that this model has 74% accuracy in predicting land cover changes on the basis of existing data. This means that 74% of the land cover changes that occur correspond to the expected outcome (Figure 3).

Erosion rate

The results of the simulation using the SWAT model for the catchment area of the Matting Das Saddang area revealed that in the 2011 simulation, the precipitation value was 1.388 mm, with a potential evapotranspiration (PET) of 1,491.2 mm, whereas the actual evapotranspiration (ET)

Table 3. Changes in land cover

Yes	Land cover	Land cover area					
		2011 Land cover (ha)	Percentage of land cover 2011 (%)	Land cover 2020 (Ha)	Land cover percentage 2020 (%)	Land cover 2030 (ha)	Percentage of land cover 2030 (%)
1	Forest	95	5	96	5	104	6
2	Shrub	505	28	521	29	488	27
3	Agriculture	399	22	442	25	519	29
4	Paddy	366	21	327	18	281	16
5	Savannah/grassland	416	24	319	19	313	18
6	Settlement		-	76	4	76	4
Total		1781	100	1781	100	1781	100

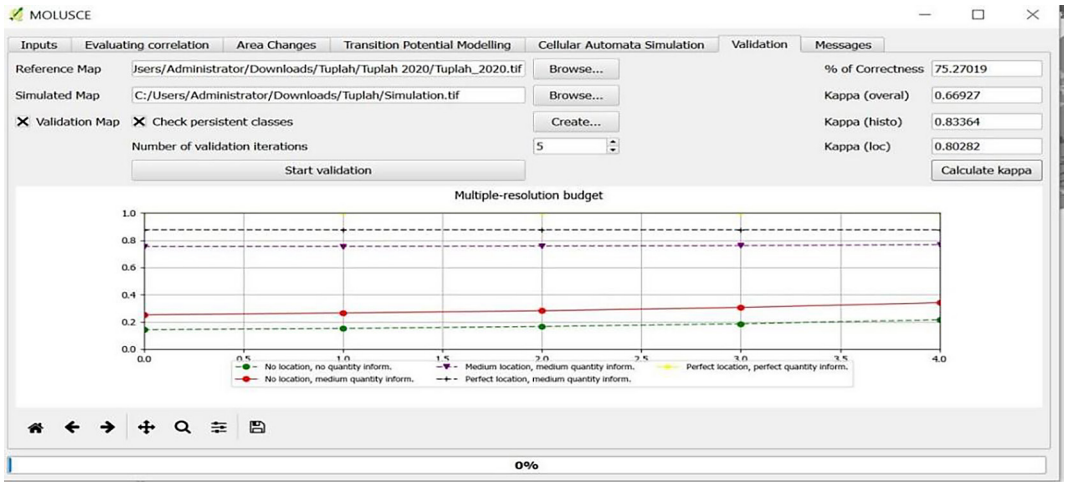

Figure 2. Land cover change validation results

Table 4. Transition matrix

Land **c**over	Forest	Shrub	Agriculture	Paddy	Savannah/ grassland	Settlement	Sum
Forest	17		5		3		25
Shrub	2	19	2		2		25
Agriculture		5	15		5		25
Paddy			3	19	3		25
Savannah/grassland		2	2	1	20		25
Settlement						10	10
Sum	22	21	33	22	27	10	135
Overall **a**ccuracy	74%						

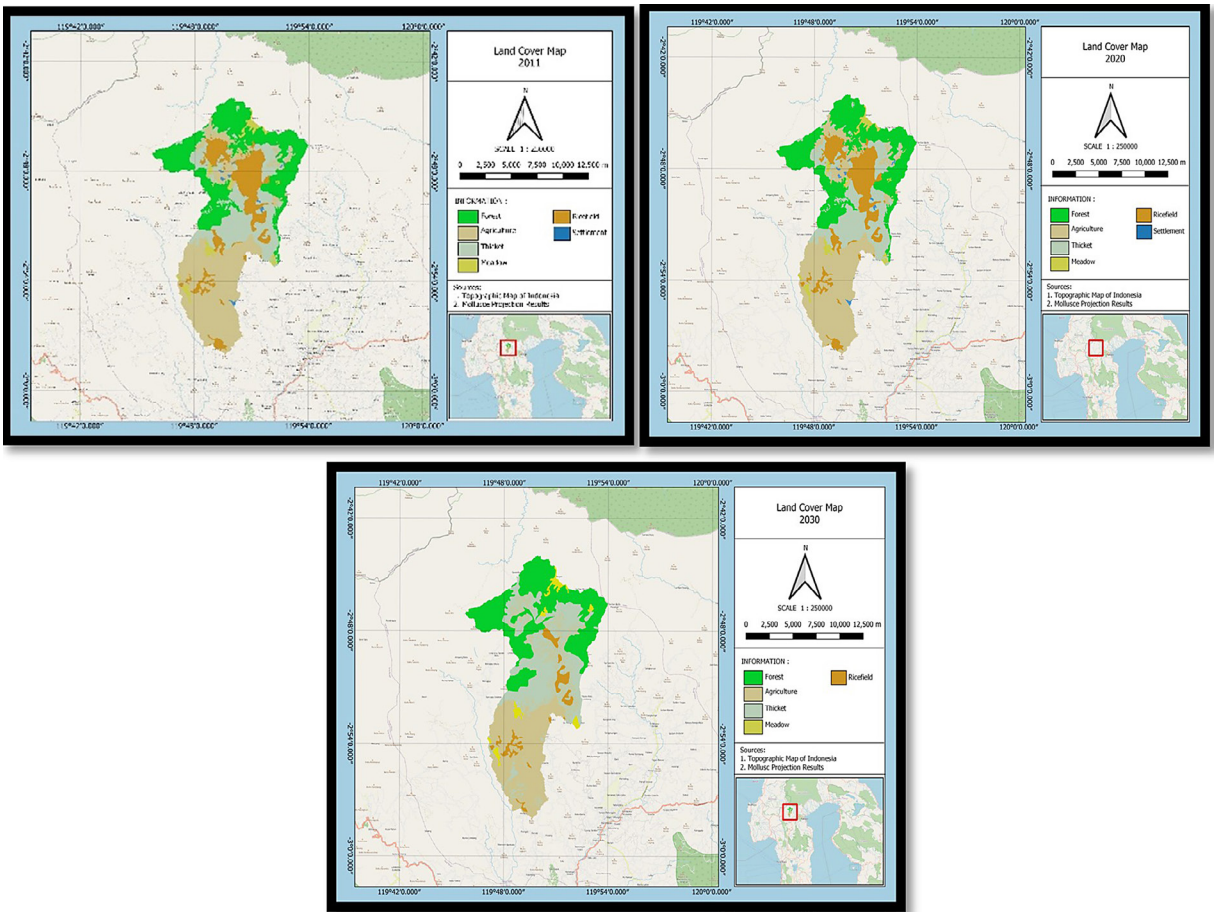

Figure 3. Land cover change

reached only 580.8 mm or approximately 42% of the annual rainfall. The surface runoff was recorded at 105.89 mm, whereas the lateral flow reached 755.92 mm, and the return flow was 14.61 mm. Percolation to shallow aquifers reaches 41.34 mm, with recharge to deep aquifers of only 2.07 mm (Figure 4).

The following simulation for 2020 revealed an increase in rainfall to 1.419 mm, whereas the PET value decreased slightly to 1,489.6 mm. The actual evapotranspiration increased to 710.4 mm or approximately 50% of the rainfall. The surface runoff value decreased drastically to 44.31 mm, indicating that a smaller amount of surface runoff occurred. The lateral flow remained high at 759.25 mm, and the return flow was recorded at 6.94 mm. Percollation decreased to 30.6 mm, and recharge to the deep aquifer was recorded at 1.53 mm. The value of the curve number decreased to 48.12, indicating an increase in the ability of the soil to infiltrate. The simulations for the 2030 projections show a similar pattern, with a rainfall of 1.436 mm and a

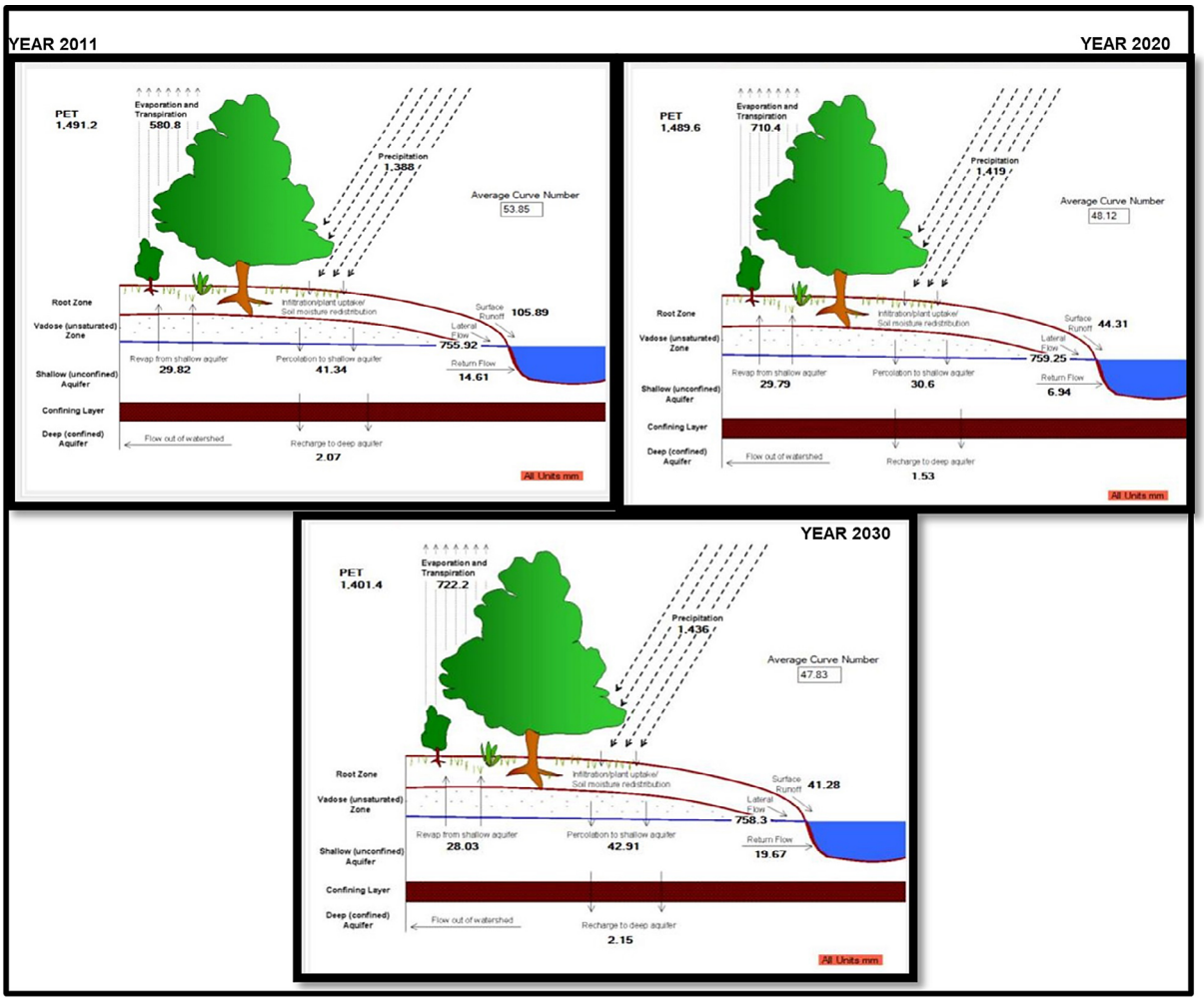

Figure 4. Hydrological simulation soil water assessment tools

PET of 1,401.4 mm. The actual evapotranspiration increased to 722.2 mm, which indicates that high vegetation activity absorbs and evaporates water. The surface runoff was recorded at 41.28 mm, the lateral flow was 758.3 mm, and the return flow was 19.67 mm. Percolation increased to 42.91 mm, and recharge to the aquifer was slightly greater than that in the previous year, at 2.15 mm. The curve number value of 47.83 strengthens the indication that the land conditions in that year strongly support water infiltration into the soil. After the hydrological simulation is generated, we can also see that the surface run simulation

For each simulation year, on the basis of the simulation results shown in Figure 5, the *surface runoff* value reached 105.89 mm/year in 2011, indicating a high surface runoff intensity in the Matting watershed. The average upland sediment yield was 20.89 Mg/ha, with a maximum value of 47.45 Mg/ha. In the second simulation for 2020, the surface runoff value decreased drastically to 44.31 mm/year, which was accompanied by a decrease in the average sediment load of upstream land to 6.21 Mg/ha, and the maximum sediment load decreased to 25.91 Mg/ha. Nevertheless, in the third simulation for the 2030 projection, the average sediment value increased to 7.75 Mg/ha, and the maximum sediment value reached 27.29 Mg/ha. The surface runoff value is also relatively small, at 41.28 mm/year. Overall, the three simulations conducted demonstrated the dynamics of sediment values, which were significantly influenced by the amount of surface runoff and land use in the Matting watershed catchment area of Saddang. The erosion hazard class map for 2011 shows that the distribution of soil erosion levels in the North Toraja Regency area is in the medium category (60--180 tons/ha/year), with yellow predominant, and there is also a dark green color that characterizes a higher erosion potential that falls into the heavy category (180--480 tons/ha/year) (Figure 6).

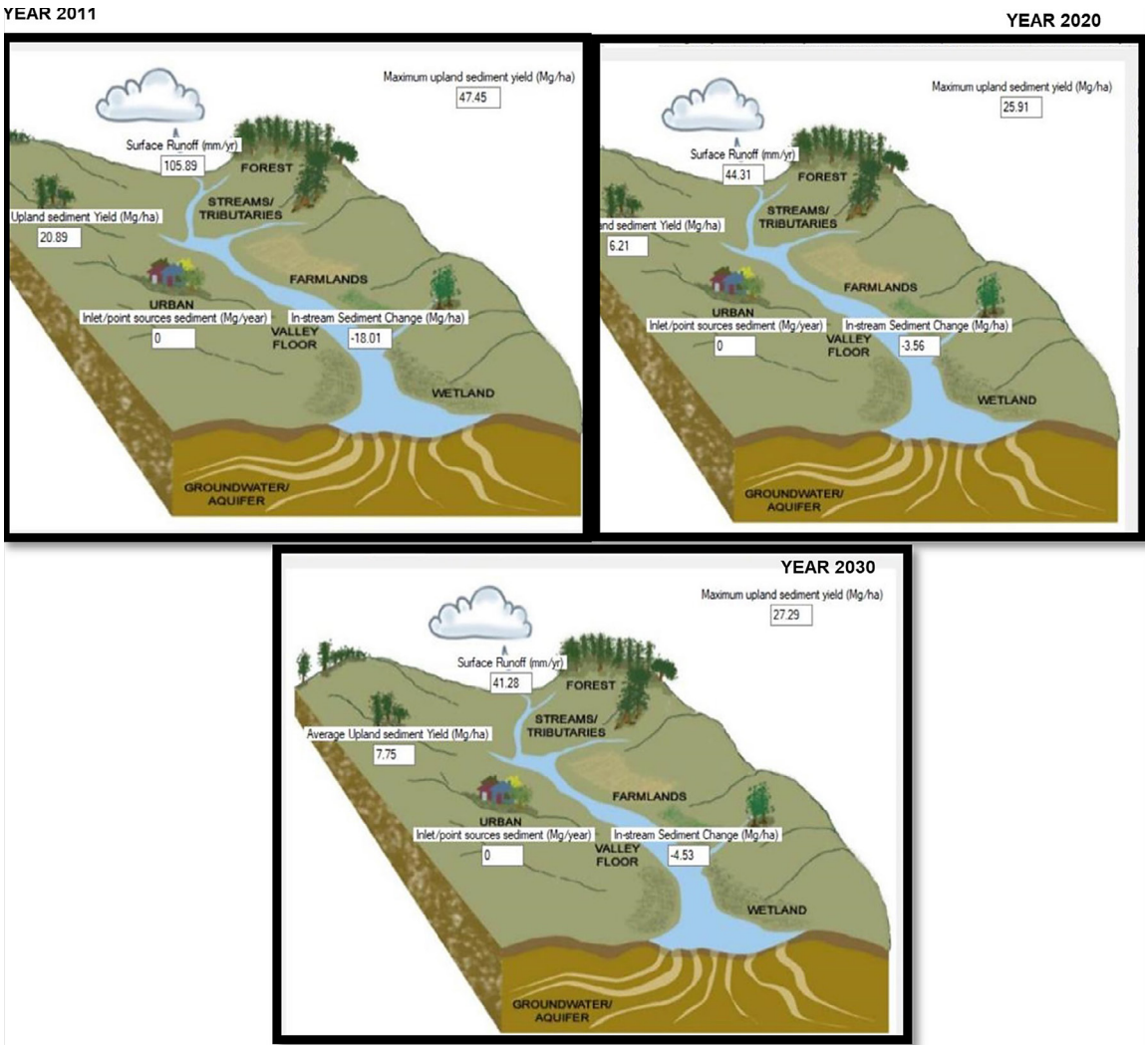

Figure 5. Surface runoff simulation

In 2011, soil erosion occurred. This shows that in 2011, the soil erosion that occurred was quite significant but did not reach a burdensome level and could not directly threaten the sustainability of the ecosystem. In contrast, the erosion hazard class in 2020 exhibited a significant change compared with that in 2011. Areas that were previously classified as heavy in 2011 are now mostly experiencing a reduction in erosion hazard, categorized as moderate. The 2030 projection map shows a more optimistic picture, where most areas in Tana Toraja Regency have succeeded in reducing the level of erosion hazard and switching to the light category (< 15 tons/ha/year). A comparison of the 2011, 2020, and 2030 projections reveals that there is a significant downward trend in the erosion hazard class, especially in areas that were previously classified into heavy and medium categories (Table 5). Class I (very light) has an erosion rate of less than 15 tons/ha/year, with a total erosion rate of 3.182 tons/ha/year. This class shows relatively stable and controlled land use conditions. These areas generally have good cover vegetation or are flat areas with a low risk of erosion. Class III (medium) has an erosion rate between 60 and 180 tons/ha/year, with a total erosion contribution of 1,656,355 tons/ha/year. This value indicates a considerable amount of pressure on the land, which is most likely due to agricultural practices on sloping land, nonpermanent land cover, and a lack of soil conservation measures. Class IV (heavy), with an erosion rate between 180 and 480 tons/ha/year. The contribution is quite significant, with a total erosion rate of 190.04 tons/ha/year. This reflects the condition of the land, which is very prone to erosion because of its high slopes and lack of vegetation cover (Table 6).

Class I (very light) covers most areas with less than 15 tons/ha/year. The total erosion rate

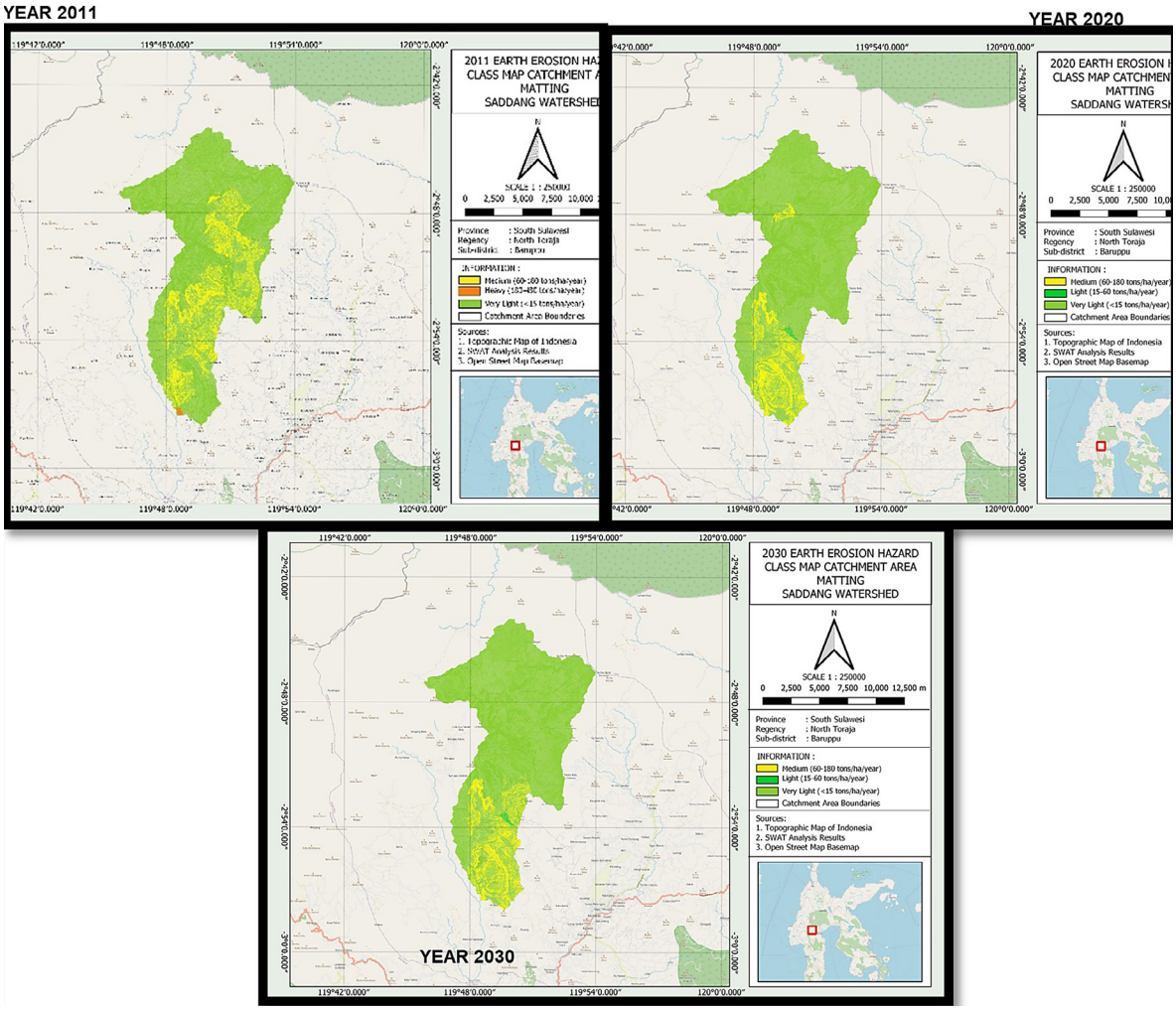

Figure 6. Erosion hazard class map

Table 5. Table of erosion rates in 2011

Erosion classes	Erosion rate range (tons/ha/year)	Description of erosion classes	Total erosion rate (tons/ha/year)
Class I	< 15	Very light	3.182
Class III	60–180	Keep	1,656.355
Class IV	180–480	Heavy	190.04

Table 6. Table of erosion rates in 2020

Erosion classes	Erosion rate range (tons/ha/year)	Description of erosion classes	Total erosion rate (tons/ha/year)
Class I	< 15	Very light	2.638
Class II	15–60	Light	52.744
Class III	60–180	Keep	454.682

for this class is 2,638 tons/ha/year, indicating that this area is in stable condition, characterized by good land cover, such as forests or natural vegetation, and is located on a low slope. Class II (lightweight) only covers an erosion rate of 52,744 tons/ha/year. Although still in the light category, this area warrants concern for preventing future erosion increases, especially in the event of land cover changes or intensification of land use. Class III (medium) encompasses erosion rates ranging

from 60 to 180 tons/ha/year. The total erosion rate in this class reached 454,682 tons/ha/year, or approximately 89% of the total erosion. This suggests that most of the erosion burden originates from areas with moderate erosion levels, likely due to a combination of factors, including steep slopes, open land, and a lack of conservation measures (Table 7).

Class I (very light) has an erosion rate of < 15 tons/ha/year. The total erosion rate in this class is 2.983 tons/ha/year. This category indicates that the land conditions are relatively stable, with adequate cover vegetation and topographic conditions that are not too steep. In Class II (light), with an erosion value of 52,744 tons/ha/year, although still in the light category, this area warrants attention because land use change or unsustainable management can lead to increased erosion. Class III (medium), with erosion rates between 60 and 180 tons/ha/year. The total erosion rate in this class reaches 454,682 tons/ha/year, or approximately 89% of the total erosion.

Table 7. Rate of erosion in 2030

Erosion classes	Erosion rate range (tons/ha/year)	Description of erosion classes	Total erosion rate (tons/ha/year)
Class I	< 15	Very light	2.983
Class II	15–60	Light	52.744
Class III	60–180	Keep	454.682

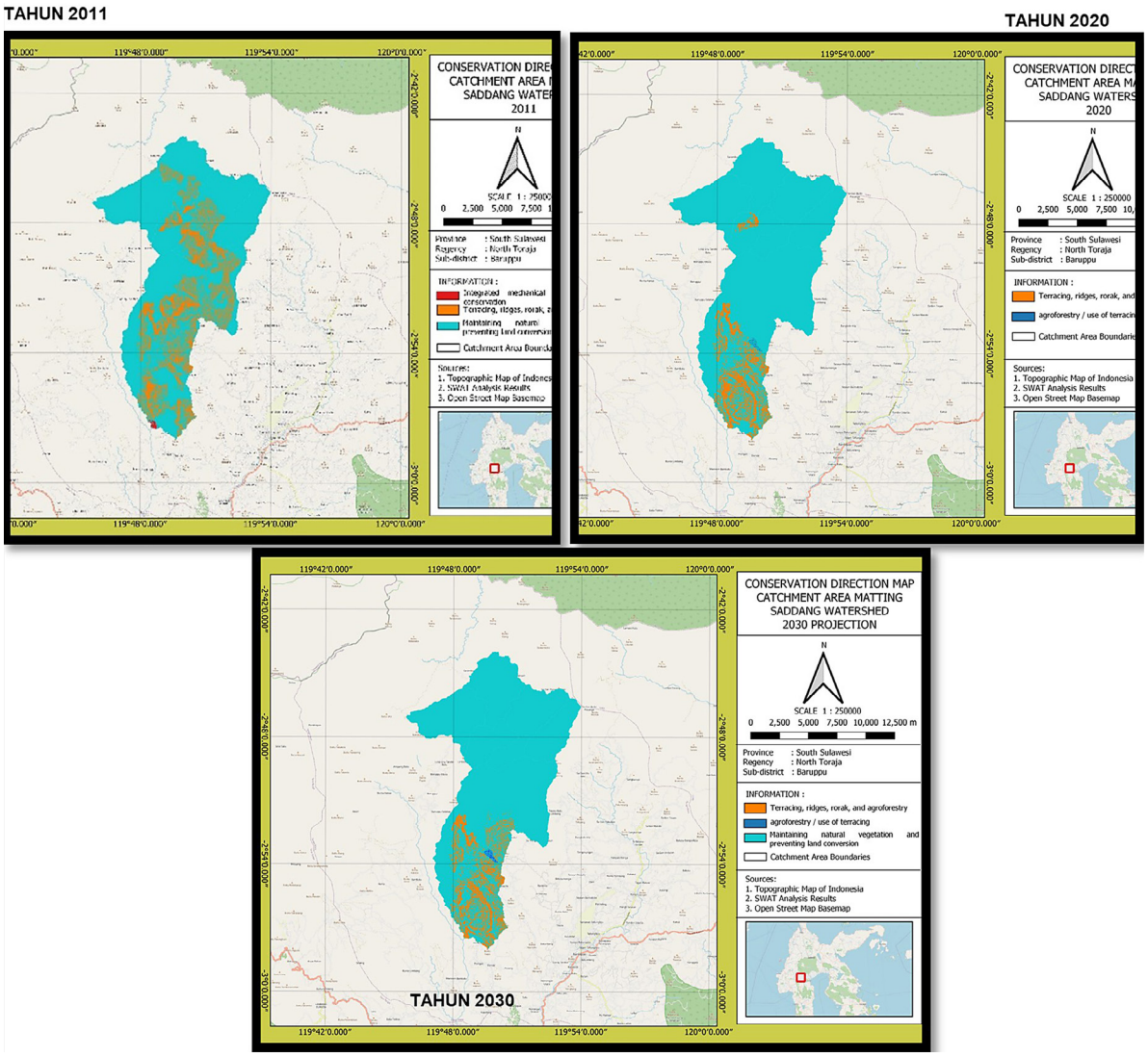

Figure 7. Land cultivation instruction map

Land cultivation instructions

The roadmaps for the 2011, 2020, and 2030 projections provide an overview of the type and intensity of recommended conservation actions on the basis of erosion conditions and land change in the region (Figure 7).

This directive aims to reduce soil erosion, improve soil quality, and maintain the sustainability of natural resources. According to the 2011 map, the wider area requires integrated mechanical and vegetation conservation, particularly in areas with steep slopes and high erosion. This reflects the need for immediate action in the regions that have suffered severe soil damage due to erosion.

On the 2020 map, most areas have improved, as indicated by the transition to natural vegetation protection and the prevention of land conversion. This finding shows that previously implemented conservation measures are starting to yield positive results in maintaining soil stability, as well as more passive conservation success, where natural vegetation is allowed to grow, thereby maintaining the ecosystem.

On the 2030 projection map, more areas are classified for agroforestry and terraces, which indicates that soil conservation is becoming more sustainable and progressive. This more intensive approach is aimed at maintaining soil quality in the long term, as well as preventing further damage to areas that are still vulnerable to erosion (PUPR, 2015).

CONCLUSIONS

Analysis of land cover changes in the Saddang watershed revealed significant changes between 2011 and 2020 and the 2030 projection. In 2011, bushes and savannas/grasslands dominated, whereas agriculture and rice paddies began to develop. Forests are still present in small proportions. The most significant change occurred in agriculture, which increased from 399 ha in 2011 to 442 ha in 2020 and is projected to be 519 ha by 2030. In contrast, rice fields have decreased, from 366 ha in 2011 to 327 ha in 2020, and are expected to decline further to 281 ha by 2030. Forests slightly increased from 95 ha in 2011 to 104 ha in 2030, reflecting the impact of conservation efforts.

The results of simulations via the SWAT model indicate a decrease in the erosion rate between 2011 and 2030. In 2011, most areas fell into the very light (Class I) category, with some subbasins experiencing moderate erosion (Class III) and one subbasin classified as Class IV (severe). In 2020, most areas previously classified in Class III switched to Class I, showing significant improvements in land management and conservation. Projections for 2030 indicate that most subbasins have reduced erosion to Class I, although some areas with steep slopes and high rainfall continue to experience moderate erosion (Class III). This reflects the success of conservation strategies, although more intensive action is still needed in the most vulnerable areas.

The land management roadmaps for 2011, 2020, and 2030 outline recommended conservation measures on the basis of erosion conditions and land changes. In 2011, areas with steep slopes and high erosion required integrated mechanical and vegetation conservation measures, such as terracing and planting ground cover vegetation, to reduce erosion. In 2020, most regions shifted their focus to preserving natural vegetation and preventing land conversion. Projections for 2030 indicate an increase in the use of agroforestry and terraces, which will ensure more sustainable soil conservation.

REFERENCES

1. Abbaspour, K. C., Vaghefi, S. A., Srinivasan, R. (2018). A guideline for successful application of the SWAT model. *Hydrological Sciences Journal, 63*(7), 1150–1171. IPB Journal.
2. Asrianto, S., Samsuar, Permata Hati, F. I. (2023). Effects of land cover change on River Discharge conditions in the Mamasa watershed using the SWAT model. *Salaga Journal, 1*(2). https://doi.org/10.70124/salaga.v1i2.1356 agritech.unhas.ac.id
3. Foody, G. M. (2020). Explaining the confusion matrix in remote sensing classification. *Remote Sensing of Environment, 239*, 111690. https://doi.org/10.1016/j.rse.2019.111690
4. Nandini, R., Kusumandari, A., Gunawan, T., Sadono, R. (2019). Assessment of land use impact on hydrological response using soil and water assessment Tool (SWAT) in Babak Watershed, Lombok Island, Indonesia. *Agriculture and Natural Resources, 53*(6), 635–642. Thai Journal Online.
5. Purwitaningsih, S., Pamungkas, A. P., Setyasa, P. T., Pamungkas, R. P., Irawan, S. A. R. (2020). Floodreduction scenario based on land use in Kedurus River Basin using SWAT hydrology model. *Geoplanning Journal, 7*(2), 87–94. https://doi.

org/10.14710/geoplanning.7.2.8794 ejournal.undip.ac.id+1ejournal.undip.ac.id+1

6. Schuol, J., Abbaspour, K. C. (2006). Calibration and uncertainty issues of SWAT in West Africa. *Advances in Geosciences, 9*, 137–143. https://doi.org/10.5194/adgeo-9-137-2006
7. Ulmas, P., Liiv, I. (2020). Segmentation of satellite imagery using U-Net models for land cover classification. arXiv preprint arXiv:2003.02899. https://arxiv.org/abs/2003.02899
8. Utomo, W. H., Arsyad, S. (2020). Soil and water conservation. *IPB Press.* https://doi.org/10.23960/jtep-l.v13i1.260-268.
9. Zhang, D., Srinivasan, R., Van Griensven, A. (2016). Cloud-based calibration/uncertainty tool for SWAT (CUT-SWAT). *Environmental Modelling & Software, 78*, 91–104. https://gmd.copernicus.org/preprints/gmd-2020-429/gmd-2020-429-ATC2.pdf.com
10. Zhu, X. X., Tuia, D., Mou, L., Xia, G. S. (2017). *Deep learning in remote sensing: A review.* https://https://arxiv.org/pdf/1710.03959
11. Abbaspour, K. C. (2005). *Calibration and uncertainty analysis of SWAT in SWAT-CUP.* https://swat.tamu.edu/media/114860/usermanual_swatcup.pdf.com
12. Ali, D. A. (2020). Using satellite imagery to assess impacts of soil and water conservation in Ethiopian watersheds. *Land Degradation & Development, 31*(2), 125–140. https://www.sciencedirect.com/science/article/abs/pii/S0921800919305257.com
13. Bappenas. (2020). *RPJMN 2020–2024: Food and Land Security Strategy*. http://journal.pusbindiklatren.bappenas.go.id/.
14. Adaptation Fund. (2019). *Community adaptation for forest-food based management in Saddang Watershed ecosystem (Technical Summary).* https://www.adaptation-fund.org/wp-content/uploads/2019/05/Indonesia-Saddang-revised_for-web.pdf.com
15. BSN. (2010). Classification of Land Closure/Use (SNI 7645:2010). *National Standardization Agency of Indonesia*. https://id.scribd.com/doc/172065064/15-SNI-7645-2010-Klasifikasi-Penutup-Lahan. Com.
16. Senanayake, S., Pradhan, B., Huete, A., Brennan, J. (2020). A review on assessing and mapping soil erosion hazard using geo-informatics technology for farming system management. *Remote Sensing, 12*(24), 4063. https://www.mdpi.com/2072-4292/12/24/4063.com
17. Vieira, C. A. O., Mather, P. M., Silva, A. S., Rodrigues, D. D., Gripp Júnior, J., Ferraz, A. S., Oliveira, J. C. (2006). Methods for assessing the positional and thematic accuracy of cartographic products in the context of remote sensing. *GeoENSEÑANZA, 11*(1), 5–15. https://www.redalyc.org/pdf/360/36012424002.pdf
18. Congalton, R. G., Green, K. (2019). *Assessing the accuracy of remotely sensed data: Principles and practices (3rd ed.).* CRC Press.
19. CUP.SWAT-CUPManual.TexasA&M University https ://swat.tamu. edu /media/ qexfwshg /05-abbaspour-france.pdf
20. Das, S. K., Li, X., Wang, Y. (2024). Calibration, validation and uncertainty analysis of a SWAT water-quality model in Yarra River, Australia. *Applied Water Science, 14*(3), 75. https://doi.org/10.1007/s13201-024-02138-x
21. Dharmawan, I. W. S., Pratiwi, S., Siregar, C. A., Narendra, B. H., Undaharta, N. K. E., Sitepu, B. S., Sukmana, A., Wiratmoko, M. D. E., Abywijaya, I. K., Sari, N. (2023). Implementation of soil and water conservation in indonesia and its impacts on biodiversity, hydrology, soil erosion and microclimate. *Applied Sciences, 13*(13), 7648. https://doi.org/10.3390/app13137648
22. Egido, A., Ruffini, G., Martín-Neira, M. (2008). *Soil moisture monitorization using GNSS reflected signals.* https://arxiv.org/abs/0805.1881
23. Food and Agriculture Organization of the United Nations. (2011). *The State of the World's Land and Water Resources for Food and Agriculture (SOLAW) – Managing Systems at Risk*. FAO. https://www.fao.org/3/i1688e/i1688e.pdf.
24. Filchev, L., Kolev, V. (2023). *Assessing of Soil Erosion Risk Through Geoinformation Sciences and Remote Sensing—a review* (arXiv preprint arXiv:2310.08430). https://arxiv.org/abs/2310.08430
25. Gasirabo, A., Musabyimana, S., Nduwayezu, E. (2023). SWAT model calibration using GLUE, ParaSol, SUFI2 in Nile Nyabarongo basin. *Frontiers in Water, 5*, 1268593. https://doi.org/10.3389/frwa.2023.1268593
26. Gaur, S., Singh, R. (2023). A comprehensive review on land use/land cover (LULC) change modeling for urban development: Current status and future prospects. *Sustainability, 15*(2), 903. https://doi.org/10.3390/su15020903
27. Sidi Almouctar, M. A., Wu, Y., Zhao, F., Dossou, J. F. (2021). Soil erosion assessment using the RUSLE model and geospatial techniques (remote sensing and GIS) in South-Central Niger (Maradi Region). *Water, 13*(24), 3511. https://doi.org/10.3390/w13243511
28. Hidayat, L., Sulistyo, B. (2019). The simulation of land use change on soil erosion and sediment transported using SWAT hydrological models in the upstream of Mrica Reservoir catchment area. https://doi.org/10.31186/terra.2.1.9-17
29. Kennedy, R. E., et al. (2009). Remote sensing change detection tools for natural resource managers. *Remote Sensing of Environment, 113*, 1382–1396. https://research.fs.usda.gov/treesearch/

download/34510.pdf.com

30. Kim, Y. I., Park, W. H., Shin, Y., Park, J.-W., Engel, B., Yun, Y.-J., Jang, W. S. (2024). Applications of machine learning and remote sensing in soil and water conservation. *Hydrology, 11*(11), Article 183. https://doi.org/10.3390/hydrology11110183
31. Nguyen, H. Q., Merz, R., Apel, H., Thang, T. D. (2018). Calibration of spatially distributed hydrological processes and model parameters in a large-scale river basin: A case study in the Day Basin, Vietnam. *Water, 10*(2), 212. https://doi.org/10.3390/w10020212
32. Cheng, G., Han, J., Lu, X. (2017). *Remote Sensing Image Scene Classification: Benchmark and State of the Art* (arXiv preprint arXiv:1703.00121). https://arxiv.org/abs/1703.00121
33. Mehari, M., Li, J., Melesse, M. (2023). Investigation of land use and land cover dynamics, drivers, and their consequences in south-central Ethiopia, with special emphasis on the contrasting agro-ecological settings of the Satame and Legabora watersheds (Preprint). https://doi.org/10.21203/rs.3.rs-2962481/v1
34. Mendoza, J. A. C., Chávez Alcázar, T. A., Zuñiga Medina, S. A. (2021). Calibration and uncertainty analysis for modelling runoff in the Tambo River Basin, Peru, using the Sequential Uncertainty Fitting Ver-2 (SUFI-2) algorithm. *Air, Soil and Water Research, 14*, Article [pendukung]. https://doi.org/10.1177/1178622120988707
35. Ministry of Environment and Forestry of the Republic of Indonesia. (2019). *Regulation of the Minister of Environment and Forestry Number 59 of 2019 concerning Planting for the Rehabilitation of River Basin Areas.* https://www.peraturan.go.id
36. Soulis, K. X. (Ed.). (2021). *Soil Conservation Service Curve Number (SCS-CN) Method: Current Applications, Remaining Challenges, and Future Perspectives* [Open access book]. MDPI. https://doi.org/10.3390/books978-3-0365-0821-4
37. Mudunuru, M. K., Son, K., Jiang, P., Chen, X. (2021). *SWAT watershed model calibration using deep learning* (arXiv preprint arXiv:2110.03097). https://arxiv.org/abs/2110.03097
38. Neitsch, S. L., Arnold, J. G., Kiniry, J. R., Williams, J. R. (2011). *Soil and Water Assessment Tool: Theoretical Documentation Version 2009 (TR-406).* Texas Water Resources Institute, Texas A&M University System. https://swat.tamu.edu/media/99192/swat2009-theory.pdf
39. Ostad-Ali-Askari, K. (2024). Calibration and uncertainty of the SWAT model using the SUFI-2 algorithm. *SSRN Electronic Journal.* https://ssrn.com/abstract=4825527 or http://dx.doi.org/10.2139/ssrn.4825527
40. Ministry of Public Works and Housing of the Republic of Indonesia. (2015). *Ministerial Regulation No. 5/PRT/M/2015 concerning General Guidelines for Implementing Sustainable Construction in Public Works and Housing Infrastructure*
41. (Ministerial Regulation No. 5/PRT/M/2015). https://peraturan. bpk.go.id/ Download/ 152402/ Permen-PUPR05-2015.pdf